Published in final edited form as:
*Anal Chem*. 2009 February 1; 81(3): 1033–1039. doi:10.1021/ac802092j.

# Enrichment of cancer cells using aptamers immobilized on a microfluidic channel

**Joseph A. Phillips**[a], **Ye Xu**[a,b], **Zheng Xia**[c], **Z. Hugh Fan**[c,d], and **Weihong Tan**[a]

a*Center for Research at the Bio/Nano Interface, Department of Chemistry and Department of Physiology and Functional Genomics, Shands Cancer Center, UF Genetics Institute, and McKnight Brain Institute, University of Florida, Gainesville, Florida 32611-7200, USA, Fax: 352-392-0346; Tel: 352-846-2410*

b*Molecular Diagnostics Laboratory, Department of Biomedical Sciences and The Key Laboratory of the Ministry of Education for Cell Biology and Tumor Cell Engineering, School of Life Sciences, Xiamen University, Xiamen, Fujian 361005, China.*

c*Department of Mechanical and Aerospace Engineering, University of Florida, P. O. Box 116250, Gainesville, FL 32611, USA.*

d*Department of Biomedical Engineering, University of Florida, P. O. Box 116131, Gainesville, FL 32611, USA. E-mail: hfan@ufl.edu*

E-mail: Joseph A. PhillipsYe XuZheng XiaZ. Hugh FanWeihong Tan [tan@chem.ufl.edu]

## Abstract

This work describes the development and investigation of an aptamer modified microfluidic device that captures rare cells to achieve a rapid assay without pre-treatment of cells. To accomplish this, aptamers are first immobilized on the surface of a poly (dimethylsiloxane) microchannel, followed by pumping a mixture of cells through the device. This process permits the use of optical microscopy to measure the cell-surface density from which we calculate the percentage of cells captured as a function of cell and aptamer concentration, flow velocity, and incubation time. This aptamer-based device was demonstrated to capture target cells with > 97% purity and > 80% efficiency. Since the cell capture assay is completed within minutes and requires no pre-treatment of cells, the device promises to play a key role in the early detection and diagnosis of cancer where rare diseased cells can first be enriched and then captured for detection.

## Introduction

Detecting cancer at its earliest stages increases the chances of positive prognosis and decreases treatment costs. An example of a simple and cost-effective method that accomplishes this objective is the widely used Pap test, in which a small sample of cells is fixed and stained for microscopic analysis (American Cancer Society, Cancer Facts & Figures 2007). Using the Pap test has, in fact, reduced the rate of incidence of cervical cancer by 70% since the 1950s. Although the Pap test can be routinely administered to women at an early age, not all tissues are as easily accessible during routine check-ups. Consequently, methods that are used to detect other cancers can be too costly to administer routinely to patients outside the established high-risk groups. One method of detecting cancers involves detecting live tumor cells in bodily fluids, i.e., sputum, urine, blood, cerebrospinal fluid, fecal blood, and body cavity fluids. In this case, the malignant cells are generally present at low concentrations. Therefore, developing

Correspondence to: Z. Hugh Fan; Weihong Tan, tan@chem.ufl.edu.

inexpensive and fast methods for enriching and detecting cancerous or pre-cancerous cells from bodily fluids is important for early detection of cancer and will lead to lower incidence of cancer-related deaths. Microfluidic devices are promising platforms that can be used to create inexpensive and fast assays for many different biological applications because of their small physical dimesnions.[1–6] These devices have already been efficiently used for some analytical measurements on whole cells. For example, several research groups have explored a variety of methods for capturing and examining single cells in microfluidic devices.[7–12] Although single cell analysis is important, we are interested in enriching rare cancer cells from a background of healthy cells. Among many approaches to this problem, one such useful method for enriching rare cells is cell-affinity chromatography.[13–15] In cell-affinity chromatography, a high affinity ligand that binds selectively to a particular cell type is immobilized on a solid support. This method, which is useful for enriching large numbers of cells in relatively short times from large volumes of samples, has recently been implemented in microfluidic devices.[16–31] These studies used antibodies as ligands. However, few highly selective and high affinity antibodies are known for each diseased cell, effectively limiting the application scope of microfluidic devices. In contrast, high affinity DNA-aptamers can be created for any cancer cell using cell-SELEX,[32–35] hence we are interested in exploiting them as high affinity ligands for cell-affinity chromatography in a microfluidic channel.

Aptamers bind selectively to a variety of targets and are obtained using a process called Systematic Evolution of Ligands by EXponential Enrichment (SELEX). Aptamers can bind to a variety of molecules, including proteins, drugs, and other small molecules, such as ATP, with dissociation constants ranging from μM to pM.[36–39] Aptamers can also distinguish between homologous proteins that contain only a few amino acid changes.[40, 41] For these reasons, aptamers have been the focus of much recent work in cancer diagnosis and therapy.[42–48] Using cell-SELEX, we have created aptamers that bind to lymphocytic and myeloid leukemia, small cell and non-small cell lung cancer, and liver cancer cells. One benefit of using aptamers derived from cell-SELEX is that these aptamers are created without explicit knowledge of the molecular difference between cancer cells and healthy cells. Therefore, cell-SELEX aptamers can be used for detection and enrichment before the corresponding antibody has been developed. We have already shown that aptamer conjugated nanoparticles can be used for detection and enrichment of cancer cells.[49, 50] Although this technique is efficient and simple, it is necessary to optimize incubating procedures, and the nanoparticle labeling may influence subsequent analysis of the extracted cells. Therefore we are interested in developing label-free detection methods to minimize sample preparation and allow cells to be analyzed by any method after the initial extraction.

We chose to base our microfluidic cell-affinity chromatography device on DNA-aptamers for many reasons. First, we will be able to generate the aptamers needed for the desired cell types of interest by using the well-developed cell-SELEX method in our lab. This cannot be done easily with other molecular recognition elements. Second, the stability of the DNA molecule makes aptamers an ideal choice for use in microfluidic devices since DNA-based devices can be stored for a long period of time and can be easily handled in clinical settings. Third, DNA aptamers can be easily modified with fluorescent or other functional moieties and can be immobilized on a variety of surfaces, giving aptamers wide applicability in their development as biosensors and medical devices.

In this work, we immobilized aptamers within a microfluidic channel and show that this surface can capture cells from a mixture of target and control cells. We investigated capture efficiency using a prototype device and then a microfabricated poly (dimethylsiloxane) (PDMS) device. We investigated the capture efficiency and purity as a function of several parameters related to device construction and operation. Using the PDMS device and the optimized cell capture assay, we obtain > 80% capture efficiency with 97% purity. This report is the first to use

aptamer-coated microchannels for cancer cell enrichment. We also investigate the pulsing of cell solutions instead of using a constant fluid flow and we analyze how reducing the channel depth leads to increased cell capture efficiency, techniques which have not been investigated in the literature.

## Experimental

### Cell Culture and Buffers

CCRF-CEM (CCL-119, T cell line, human ALL) cell line was obtained from American Type Culture Collection, and NB-4 cell line was obtained from the Department of Pathology at the University of Florida. Both cell types were cultured in RPMI medium 1640 (American Type Culture Collection) supplemented with 10% FBS (heat-inactivated; GIBCO) and 100 units/mL penicillin-streptomycin (Cellgro). Immediately before experiments, cells were rinsed with washing buffer [4.5 g/L glucose and 5 mM $MgCl_2$ in Dulbecco's PBS with calcium chloride and magnesium chloride (Sigma)] and re-suspended at 1,000,000 cell/mL. Following manufacturer's instructions, cells were treated with Vybrant DiI or Vybrant DiO cell-labeling solutions (Invitrogen) for 5 minutes at 37°C, rinsed with washing buffer and re-suspended at 10,000,000 cell/mL in binding buffer [washing buffer supplemented with yeast tRNA (0.1 mg/mL; Sigma), BSA (1 mg/mL; Fisher), and 10% FBS]. Labeled cells were stored on ice and further diluted before experiments.

### Device Fabrication and Operation

Prototype devices were fabricated as follows. Microscope slides and 18 mm square No. 1 cover glasses (Fisher) were rinsed with deionized $H_2O$ and dried under nitrogen. Strips of double-sided tape (3M) were placed 4 mm apart on a microscope slide, and a cover glass was placed on top. Devices were filled by capillary action. Solution exchange was performed by simultaneously pipetting solution at one end and withdrawing fluid from the other end with P8 filter paper (Fisher).[51] Poly(dimethylsiloxane) devices were fabricated using a process similar to what is described in the literature.[52] The layout of the device was designed in AutoCAD and printed on a transparency using a high-resolution printer. The pattern on the transparency was transferred to a silicon wafer via photolithography. The silicon wafer was etched to a depth of 25 μm in a deep reactive ion etching machine. The resulting silicon wafer with the desired pattern served as a mold to fabricate a number of PDMS devices. Sylgard 184 (Corning) reagents were prepared and thoroughly mixed by following the manufacturer's instructions. After being degassed to remove bubbles, the mixture was cast on top of the silicon mold. After being cured at room temperature, the PDMS layer was peeled off the silicon mold. Inlet and outlet wells were created at the channel ends by punching holes in the PDMS. The PDMS slice was reversibly attached to a clean 50 × 45 mm No. 1 cover glass (Fisher) to form a device. Avidin and DNA solutions were introduced into channels by applying a vacuum to one end of the channel. After channel surfaces were modified as discussed in the next section, cell solutions were introduced into the channel by connecting a Micro4 syringe pump (World Precision Instruments, Inc.) to the outlet of the channel. In between experiments, PDMS devices were cleaned by sequential sonication in 20% bleach with 0.1 M NaCl and then 50:1 water:versaclean (Fisher) at 40°C, followed by rinsing in deionized $H_2O$ and drying under $N_2$.

### Cell Capture Assay

One channel volume of avidin at 1 mg/mL (Invitrogen) in phosphate buffered saline was incubated in the device for 15 seconds and rinsed with 3 channel volumes of binding buffer. One channel volume of biotinylated DNA was then incubated for 15 seconds and rinsed with 3 channel volumes of binding buffer. Dye-labeled cells were mixed together and diluted to specific concentrations in binding buffer with 10% FBS. To avoid cell settling that would

otherwise occur with a syringe, cell solutions were dropped onto the inlet of the device with a pipette.[19] Pulses of one channel volume of cell solution were incubated for a specified time until a total of 48 μL was passed through the device, at which point a final rinse with 3 channel volumes of binding buffer was performed before imaging. Experiments were done in triplicate, and the reported error is the average error or the standard deviation, whichever is larger. Unless otherwise stated, cell concentrations were between 500,000 cell/mL and 1,000,000 cell/mL.

### Microscopy, Image Analysis, and Flow Cytometry

In order to determine the cell surface density, sets of three images corresponding to the red fluorescent target cells, green fluorescent control cells, and the transmission image were obtained at 10 positions along the channel. Images were imported into ImageJ (NIH), the threshold was set to highlight fluorescent cells, and cell counts were obtained using the Analyze Particles function. Cell counts were further confirmed by comparing fluorescent images with transmission images to verify cell morphology. The number of total cells captured was calculated by multiplying the average cell surface density by the surface area of the channel. To determine the exact concentration of both cell types used during each experiment, cell solutions were placed on a hemacytometer (Fisher), and 9 image sets were obtained. Images were imported into ImageJ, each cell type was counted manually, and the cell concentration was calculated according to the manufacturer's instructions. The capture percentage was calculated by dividing the total number of cells pumped through the device by the total cells captured. Loss of cells at the device inlet was not taken into account. Devices and hemacytometer were imaged using an Olympus FV500-IX81 confocal microscope. Flow cytometry was performed with a FACScan cytometer (BD Immunocytometry Systems). Briefly, 1,000,000 cells were incubated with fluorescent-labeled DNA at 250 nM for 15 minutes in binding buffer with 10% FBS, and 30,000 counts were measured in the flow cytometer.

### DNA synthesis

The aptamer sgc8 sequence, FAM-5'-ATC TAA CTG CTG CGC CGC CGG GAA AAT ACT GTA CGG TTA GAT TTT TTT TTT -3'-biotin, and the random DNA sequence, FAM-5-'ATT ACC TCT AAA TCA CTG CTC TGT AAC ATG GTC GCG CTA GGT TTT TTT TTT-3'-biotin, were synthesized using an ABI3400 DNA/RNA synthesizer (Applied Biosystems). DNA synthesis reagents were purchased from Glen Research (Sterling, VA). DNA purification was performed with a ProStar HPLC (Varian) using a C18 column (Econosil, 5U, 250 × 4.6 mm) from Alltech Associates. UV-Vis measurements were performed with a Cary Bio-300 UV spectrometer (Varian) to measure DNA concentration.

## Results and Discussion

### DNA aptamers

We chose to use DNA aptamers derived from cell-SELEX for the microfluidic device. We first used aptamer sgc8 that specifically binds to the T-cell Acute Lymphocytic Leukemia cell line, CCRF-CEM (target), with $K_d$ = 0.8 nM, as reported previously.[32] The sgc8 sequence was shortened and further modified with a polyT(10) linker to enhance function after binding to the glass surface.[53–55] A biotin moiety was incorporated at the 3' end so that the aptamer could be immobilized within a microfluidic channel via the biotin-avidin interaction. Finally, a fluorescein (FAM) was added at the 5' end for visualization. The exact DNA sequences used in this work are given in the experimental section. Two negative controls were designed to analyze the specific binding of the modified sgc8 aptamer. First, a random DNA sequence was chosen and also modified with polyT(10), biotin, and FAM. Second, a control cell line, NB-4 (control), which does not bind to sgc8, was used to study nonspecific binding.

Although not common, it is possible that the modifications to the aptamer sequence discussed above can have deleterious effects on the binding properties. Therefore, to ascertain whether the modified sgc8 sequence could still selectively bind to cells in solution, we performed flow cytometry and confocal microscopy on target and control cells. Saturating concentrations of sgc8 and the random sequence were incubated separately with target and control cells as described in the Microscopy and Image Analysis section. Aliquots of each cell solution were plated on a microscope slide for fluorescent microscopy and the remaining solutions were analyzed using flow cytometry. Representative fluorescence and transmission image pairs of the four combinations of cells and DNA show that the aptamer selectively binds to target cells (see Figure 1). A significant fluorescent signal covering the entire cell is seen only for sgc8 and target cells (Figure 1A), signifying the specific binding of sgc8 to target cells. In contrast, the control cells show no observable difference between the aptamer (Figure 1C) and the random sequence (Figure 1D). These images suggest an increase in binding of sgc8 to target cells when compared to the random DNA control sequence using confocal microscopy. To confirm these results, we used flow cytometry to analyze the same cell preparation. The flow cytometry analysis shows an increase in the fluorescent signal for the sgc8-stained target cells when compared to random-DNA stained target cells (Figure 1E). There was no increase in the signal for sgc8 stained control cells relative to random-DNA (Figure 1F). The flow cytometry data correlate with the fluorescent images and show that the selective aptamer staining is statistically significant, since 30,000 cells were counted to create these graphs. These experiments show that the modifications made to the aptamer do not interfere with the specific selectivity towards its target cell line.

## Aptamer-immobilized glass surface

Since the modified sgc8 can still bind selectively to target cells, we constructed prototype devices to investigate the efficacy of cell capture on an aptamer-coated glass surface. Prototype devices are constructed by sandwiching two pieces of double-sided tape between a microscope slide and a glass cover slip. These devices hold 8 μL and are roughly 4 × 18 × 0.1 mm in dimension. To create the aptamer coating, avidin is first incubated within the device and allowed to adsorb to the clean glass surface. Then biotinylated DNA and cell solutions are sequentially pumped through the device (Figure 2A). To clearly show the selectivity of the aptamer-immobilized microfluidic channels, we pumped separate solutions of target and control cells, at a concentration of 1,000,000 cell/mL, through devices that had either sgc8, or random DNA immobilized. For ease of visualization, we first stained cells with a fluorescent membrane staining dye. In these experiments, the target cells were captured at 212 ± 12 cell/mm$^2$ on the sgc8 immobilized surface (Figure 2B). Experiments using control cells and sgc8 showed cells captured at 2 ± 1 cell/mm$^2$ (Figure 2C). These results show an improvement of more than 2 orders of magnitude in the aptamer's selectivity of target cells over control cells. Control experiments using the random DNA sequence captured target cells at 7 ± 2 cell/mm$^2$ and control cells at 4 ± 1 cell/mm$^2$ (Figure 2D and 2E, respectively). This shows that it is the specific aptamer sequence that can selectively bind to target cells and not the inherent nature of a DNA coated surface. Repeat experiments using no fluorescent membrane stain and a different fluorescent membrane stain showed similar results, meaning that the membrane stain that we use for visualization has no effect on aptamer binding (data not shown). These results verify that the polyT(10) linker is adequate to allow the sgc8 aptamer to selectively bind the target cells when immobilized on the avidin-modified glass surface.

## Concentration effects

Having established that immobilized aptamers bind selectively to their target cells on an aptamer-coated glass surface, we performed experiments to analyze the effect of cell concentration on cell capture efficiency of the prototype device. In these experiments, target and control cells are treated with different fluorescent membrane stains and mixed together

prior to the start of the experiment in order to mimic a heterogeneous state of diseased and healthy cells, as seen in tumors. We varied cell concentrations from 200,000 cell/mL to 2,000,000 cell/mL, and the cell surface density grew linearly with the increased cell concentration (Figure 3A). Further, the percentage of cells captured did not change within this concentration range (Figure 3B). This result suggests that the device has a large dynamic range to capture cells for analysis and that the capture efficiency in the device is independent of cell concentration within this range. In all of these experiments, the purity of captured target cells was > 95%, the capture efficiency of control cells was less than 0.7%, and the capture efficiency of target cells was greater than 15%. To further understand the parameters on which cell capture depends, we investigated the incubation time used for cell immobilization and the DNA concentration used during aptamer immobilization.

## Parameters affecting capture efficiency

In the previous experiments that analyzed cell capture versus cell concentration, we used a fixed DNA concentration of 20 μM during the aptamer immobilization step. Since the DNA concentration used in this step determines the aptamer surface density, we investigated how the device responded when different DNA concentrations are used during aptamer immobilization. The target cell capture percentage increased rapidly above 400 nM and almost saturated at 50 μM (Figure 3C). These data show that the surface density of the aptamer affects the performance of the device. In these experiments, we observed that 1) the control cells were captured at less than 0.3%, 2) target cells were captured at a percentage ranging from 9% – 15%, and 3) the purity of captured target cells was > 96%, except for the experiment using 400 nM DNA in which the purity fell to 75%.

We also tested the incubation time used during cell capture in the microfluidic device. In all previous experiments, the incubation time for cell capture was 30 seconds. This incubation step aids in the immobilization of cells by increasing their residence time within the device and allowing the cells to interact with the aptamer-coated surface at zero velocity. We varied this incubation time from 2 minutes to 0 seconds. In the 0 second experiment, the full 48 μL of cell solution was passed directly through the device in one pulse. The results showed that cell capture increases linearly with the incubation time (Figure 3D). Although control cell capture also increases linearly with incubation time, the capture percentage remains below 1.5% with a purity for target cells > 95%, even for the 2-minute incubation. These results show that the capture efficiency can be fine tuned by varying the aptamer surface density and cell residence time. This tuning capability will be useful in future applications in which the parameters used to operate the device are specified by requirements other than cell capture efficiency.

## PDMS Microfluidic Device

After performing these various experiments, we designed a PDMS channel with dimensions 4 × 25 × 0.025 mm, which is similar in width and length to the prototype, but four times more shallow in depth. Based on the results described above, we hypothesized that cells would have a higher probability of interacting with the aptamer-coated surface if channel height were to be decreased, thus increasing cell capture efficiency. The PDMS device incorporates this design principle. A further benefit of the PDMS device is that input and output ports are easily connected to a syringe pump allowing reproducible flow rates (Figure 4A). The only change to the cell capture assay when using the PDMS device is that the 48 μL of cell solution is passed through the device using 3 μL pulses. Since the pumping is automated using the syringe pump, the entire experiment could be visualized microscopically (see supplemental cell capture movie). Images of the initial cell mixture, with target cells stained red and control cells stained green, show that both cell types are uniformly dispersed and at the same concentration (Figure 4B). However, the target cells dominate the population of captured cells, indicating effective

and selective cell capture of the aptamer (Figure 4C). By comparing image pairs taken at 20 second intervals, it is possible to count the number of cells that are captured on the surface over the course of the cell capture assay. This analysis reveals that the target cell surface density increases linearly with time, whereas the control cell surface density remains constant. Using the syringe pump to accurately control the flow rate, we investigated the effects of fluid flow rate on cell capture efficiency. These experiments show that target cell capture increases with decreasing flow rate and that the PDMS device reaches > 80% target capture efficiency with ~ 97% purity of captured target cells below 200 nL/sec. However, the purity decreases to 86% at the slowest measured flow rate, indicating that nonspecific binding increases as flow rates decrease below 150 nL/second. These results show a strong dependence of cell capture efficiency on fluid flow rate and that an optimum flow rate can be found that has the best capture efficiency with the least amount of non-specific binding. This optimal flow rate and the shear force it exerts on captured cells should scale with the aptamer binding affinity and the number of receptors on the cell surface that are bound to the channel wall.[16, 18, 19, 28, 29] In future applications, the difference in shear force necessary to break the cell-surface bond of cells captured with different aptamers could be used to perform cell sorting.

When comparing the results between prototype and PDMS devices, the decreased depth of the PDMS device has a significant effect on cell capture efficiency. After adjusting for channel length, the capture efficiency increased from 12% in the prototype devices to 58% in the PDMS devices under the same conditions. This increased capture efficiency cannot be due to diffusion or convection processes within the channel. The relative strength of these processes can be estimated by calculating the Peclet number, which is the ratio of convectional to diffusive mixing, *Pe* = (Fluid Velocity) × (Characteristic Length of Flow) ÷ (Cell Diffusivity).[56] Here the cell diffusivity can be estimated by using the Einstein relation, and Stokes' law at low Reynolds number. This analysis yields Pe ~ $10^5$ for both devices, meaning that convectional mixing dominates, but that cells must travel several meters before significant mixing occurs. It is possible that some microfluidic effect causes the cells to deviate from the fluid flow and move towards the walls of the device. Mathematical modeling of spheroid particles moving at low Reynolds number in a parallel plate device shows that spheriods can move towards the walls.[57] This analysis showed that if the diameter of the particle is on the order of the channel height, then the velocity perpendicular to the fluid flow is 2–3 orders of magnitude slower than the maximum fluid velocity within the channel. We can apply this theory to the PDMS device because the channel height is approximately twice the cell diameter. For the flow rates used in this study, the maximum fluid velocities range from 750 – 5400 μm/sec, yielding perpendicular velocities of 1–50 μm/sec, allowing the cells to traverse the 25 μm channel during the cell pulse interval. This mechanism would increase the collision rate between cells and the aptamer-coated surface, thereby increasing the capture efficiency.

## Conclusion

The two main challenges for detecting rare cells are enrichment and subsequent detection. Our device overcomes the first challenge by implementing a high surface area-to-volume ratio that increases the collision rate between the target cells and the capture surface. We have shown that aptamers immobilized within a microfluidic channel can quickly and efficiently enrich cancer cells from a background of control cells. The percentage of captured cells is consistent with methods that utilize antibodies as high affinity ligands.[16–31] Using the PDMS device with optimized assay parameters, roughly 50,000 target cells are captured in 6 minutes from a 50 μL sample (500,000 cell/hr). Although this throughput is not yet optimized for patient samples, the device can be modified to accommodate larger sample volumes by increasing the channel length, having multiple channels, or implementing novel channel geometries. In addition, we may incorporate micro-pillars or other micro-features to enhance surface area and thus capture efficiency as demonstrated recently.[25, 30, 31, 58] Our work does not address the

second challenge of detecting captured cells, since using a microscope to scan the entirety of a microfluidic device is not practical. The most likely methods of detection will involve biochemical assays which have been designed to detect disease specific differences in rare cells that would have otherwise gone unnoticed in the initial patient sample.[26] These microfluidic enrichment schemes are fast, cheap, do not require lasers or other expensive equipment to operate, and have minimal sample preparation steps. Therefore, these devices will be useful for early diagnosis of cancer where it is essential to probe patients early in life and at regular intervals.

Aptamers have been used to capture eukaryotic and prokaryotic cells on a surface; however, to our knowledge, this is the first use of aptamer-coated microchannels for cancer cell enrichment.[59, 60] Also, no devices have used the pulsing of cell solutions, which allows the operation of the device at higher flow rates, and little work has been done to analyze how reducing the channel depth leads to increased cell capture efficiency. Since aptamers can be created for any diseased cells, we believe that the integration of aptamers as high affinity molecular probes into microfluidic cell capture devices will broaden the applicability and diversity of microfluidic cell-affinity chromatography devices. Future work will focus on using multiple aptamers for multiplexed detection of cancer cells, creating novel microfluidic architectures to enhance detection efficiency and sample throughput, and implementing single cell analysis on captured cells to perform biochemical assays on clinical samples.

## Supplementary Material

Refer to Web version on PubMed Central for supplementary material.

## Acknowledgements

This work was supported by NSF and NIH grants.

## References

1. Das C, Fredrickson CK, Xia Z, Fan ZH. Sens. Actuators, A 2007;134:271–277.
2. Situma C, Hashimoto M, Soper S. Biomolecular Engineering 2006;23:213–231. [PubMed: 16905357]
3. Witek MA, Wei S, Vaidya B, Adams AA, Zhu L, Stryjewski W, McCarley RL, Soper SA. Lab Chip 2004;4:464–472. [PubMed: 15472730]
4. Yi C, Li C, Ji S, Yang M. Anal. Chim. Acta 2006;560:1–23.
5. Lui RH, Yang J, Lenigk R, Bonanno J, Grodzinski P. Anal. Chem 2004;76:1824–1831. [PubMed: 15053639]
6. Furdui VI, Harrison DJ. Lab Chip 2004;4:614–618. [PubMed: 15570374]
7. Bontoux N, Dauphinot L, Vitalis T, Studer V, Chen Y, Rossier J, Potier M-C. Lab Chip 2008;8:443–450. [PubMed: 18305863]
8. James CD, Reuel N, Lee ES, Davalos RV, Mani SS, Carroll-Portillo A, Rebeil R, Martino A, Apblett CA. Biosens. Bioelectron 2008;23:845–851. [PubMed: 17933506]
9. Jang L-S, Wang M-H. Biomed. Microdevices 2007;9:737–743. [PubMed: 17508285]
10. Koschwanez JH, Carlson RH, Meldrum DR. Rev. Sci. Instrum 2007;78044301.
11. Toriello NM, Douglas ES, Mathies RA. Anal. Chem 2005;77:6935–6941. [PubMed: 16255592]
12. Yun K-S, Yoon E. Biomed. Microdevices 2005;7:35–40. [PubMed: 15834518]
13. Putnam DD, Namasivayam V, Burns MA. Biotechnol. Bioeng 2003;81:650–665. [PubMed: 12529879]
14. Mandrusov E, Houng A, Klein E, Leonard EF. Biotechnol. Prog 1995;11:208–213. [PubMed: 7766103]
15. Triebel F, Gluckman JC, Chapuis F, Charron D, Debre P. Immunology 1985;54:241–247. [PubMed: 3871417]

16. Cheng X, Irimia D, Dixon M, Sekine K, Demirci U, Zamir L, Tompkins RG, Rodriguez W, Toner M. Lab Chip 2007;7:170–178. [PubMed: 17268618]
17. Wang K, Marshall MK, Garza G, Pappas D. Anal. Chem 2008;80:2118–2124. [PubMed: 18288818]
18. Plouffe BD, Njoka DN, Harris J, Liao J, Horick NK, Radisic M, Murthy SK. Langmuir 2007;23:5050–5055. [PubMed: 17373836]
19. Plouffe BD, Radisic M, Murthy SK. Lab Chip 2008;8:462–472. [PubMed: 18305866]
20. Du Z, Colls N, Cheng KH, Vaughn MW, Gollahon L. Biosens. Bioelectron 2006;21:1991–1995. [PubMed: 16242927]
21. Du Z, Cheng KH, Vaughn MW, Collie NL, Gollahon LS. Biomed. Microdevices 2007;9:35–42. [PubMed: 17103049]
22. Zheng T, Yu H, Alexander CM, Beebe DJ, Smith LM. Biomed. Microdevices 2007;9:611–617. [PubMed: 17516171]
23. Wojciechowski JC, Narasipura SD, Charles N, Mickelsen D, Rana K, Blair ML, King MR. British Journal of Haematology 2008;140:673–681. [PubMed: 18218048]
24. Narasipura SD, Wojciechowski JC, Charles N, Liesveld JL, King MR. Clin. Chem 2008;54:77–85. [PubMed: 18024531]
25. Nagrath S, Sequist LV, Maheswaran S, Bell DW, Irimia D, Ulkus L, Smith MR, Kwak EL, Digumarthy S, Muzikansky A, Ryan P, Balis UJ, Tompkins RG, Haber DA, Toner M. Nature 2007;450:1235–1239. [PubMed: 18097410]
26. Maheswaran S, Sequist LV, Nagrath S, Ulkus L, Brannigan B, Collura CV, Inserra E, Diederichs S, Iafrate JA, Bell DW, Digumarthy S, Muzikansky A, Irimia D, Settleman J, Tompkins RG, Lynch TJ, Toner M, Haber DA. N. Engl. J. Med 2008;359:366–377. [PubMed: 18596266]
27. Wolf M, Zimmermann M, Delamarche E, Hunziker P. Biomed. Microdevices 2007;9:135–141. [PubMed: 17123164]
28. Murthy SK, Sin A, Tompkins RG, Toner M. Langmuir 2004;20:11649–11655. [PubMed: 15595794]
29. Sin A, Murthy SK, Revzin A, Tompkins RG, Toner M. Biotechnol. Bioeng 2005;91:816–826. [PubMed: 16037988]
30. Kwon KW, Choi SS, Lee SH, Kim B, Lee SN, Park MC, Kim P, Hwang SY, Suh KY. Lab Chip 2007;7:1462–1468.
31. Chang WC, Lee LP, Liepmann D. Lab Chip 2005;5:64–73. [PubMed: 15616742]
32. Shangguan D, Li Y, Tang Z, Cao ZC, Chen HW, Mallikaratchy P, Sefah K, Yang CJ, Tan W. Proc. Natl. Acad. Sci. U.S.A 2006;103:11838–11843. [PubMed: 16873550]
33. Tang Z, Shangguan D, Wang K, Shi H, Sefah K, Mallikaratchy P, Chen HW, Li Y, Tan W. Anal. Chem 2007;79:4900–4907. [PubMed: 17530817]
34. Shangguan D, Meng L, Cao ZC, Xiao Z, Fang X, Li Y, Cardona D, Witek RP, Liu C, Tan W. Anal. Chem 2008;80:721–728. [PubMed: 18177018]
35. Chen HW, Medley CD, Sefah K, Shangguan D, Tang Z, Meng L, Smith JE, Tan W. ChemMedChem 2008;3:991–1001. [PubMed: 18338423]
36. Jhaveri S, Rajendran M, Ellington AD. Nat. Biotechnol 2000;18:1293–1297. [PubMed: 11101810]
37. Pestourie C, Tavitian B, Duconge F. Biochimie 2005;87:921–930. [PubMed: 15963620]
38. Cerchia L, Duconge F, Pestourie C, Boulay J, Aissouni Y, Gombert K, Tavitian B, de Franciscis V, Libri D. PloS Biology 2005;3:697.
39. Proske D, Blank M, Buhmann R, Resch A. Appl. Microbiol. Biotechnol 2005;69:367–374. [PubMed: 16283295]
40. Hirao I, Spingola M, Peabody D, Ellington AD. Molecular Diversity 1998;4:75–89. [PubMed: 10425631]
41. Conrad R, Keranen LM, Ellington AD, Newton AC. J. Bio. Chem 1994;269:32051–32054. [PubMed: 7528207]
42. Huang C, Cao Z, Chang H, Tan W. Anal. Chem 2004;76:6973–6981. [PubMed: 15571349]
43. Vicens MC, Sen A, Vanderlaan A, Drake TJ, Tan W. ChemBioChem 2005;6:900–907. [PubMed: 15812865]
44. Cao Z, Tan W. Chem. Euro. J 2005;11:4502–4508.

45. Cao Z, Huang C, Tan W. Anal. Chem 2006;78:1478–1484. [PubMed: 16503597]
46. Mi J, Zhang X, Rabbani ZN, Liu Y, Reddy SK, Su Z, Salahuddin FK, Viles K, Giangrande PH, Dewhirst MW, Sullenger BA, Kontos CD, Clary BM. Molecular Therapy 2008;16:66–73. [PubMed: 17912235]
47. Ferreira CSM, Papamichael K, Guilbault G, Schwarzacher T, Gariepy J, Missailidis S. Anal. Bioanal. Chem 2008;390:1039–1050. [PubMed: 17694298]
48. Soundararajan S, Chen W, Spicer EK, Courtenay-Lick N, Fernandes DJ. Cancer Res 2008;68:2358–2365. [PubMed: 18381443]
49. Herr JK, Smith JE, Medley CD, Shangguan D, Tan W. Anal. Chem 2006;78:2918–2924. [PubMed: 16642976]
50. Smith JE, Medley CD, Tang Z, Shangguan D, Lofton C, Tan W. Anal. Chem 2007;79:3075–3082. [PubMed: 17348633]
51. Howard J, Hunt AJ, Baek S. Methods Cell Biol 1993;39:137–147. [PubMed: 8246794]
52. Duffy DC, McDonald JC, Schueller OJA, Whitesides GM. Anal. Chem 1998;70:4974–4984.
53. Shangguan D, Tang Z, Mallikaratchy P, Xiao Z, Tan W. ChemBioChem 2007;8:603–606. [PubMed: 17373017]
54. Guo Z, Guilfoyle RA, Thiel AJ, Wang R, Smith LM. Nucleic Acids Res 1994;22:5456–5465. [PubMed: 7816638]
55. Yao G, Tan W. Anal. Biochem 2004;331:216–223. [PubMed: 15265725]
56. Stroock AD, Dertinger SKW, Ajdari A, Mezic I, Stone HA, Whitesides GM. Science 2002;295:647–651. [PubMed: 11809963]
57. Staben ME, Zinchenko AZ, Davis RH. Physics of Fluids 2003;15:1711–1733.
58. Adams AA, Okagbare PI, Feng J, Hupert ML, Patterson D, Gottert J, McCarley RL, Nikitopoulos D, Murphy MC, Soper SA. J. Am. Chem. Soc 2008;130:8633–8641. [PubMed: 18557614]
59. Di Giusto DA, Knox SM, Lai Y, Tyrelle GD, Aung MT, King GC. ChemBioChem 2006;7:535–544. [PubMed: 16482500]
60. Hamula CLA, Zhang H, Guan LL, Li XF, Le XC. Anal. Chem 2008;80:7812–7819. [PubMed: 18803393]

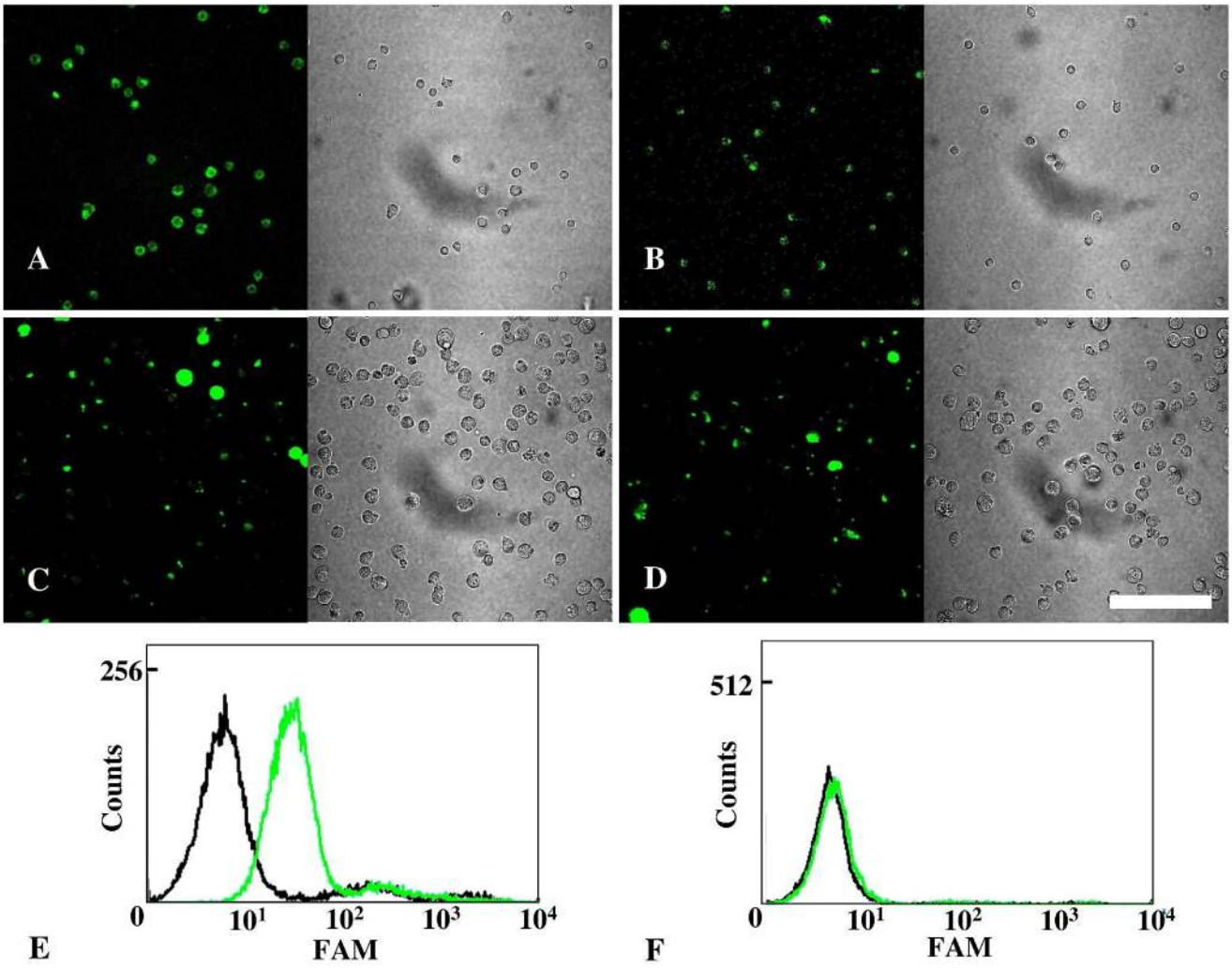


**Fig. 1.**

Selective binding of aptamers to target cells in solution using confocal microscopy and flow cytometry. Fluorescence and transmission image pairs of target cells stained with sgc8 (A); target cells stained with random DNA (B); control cells stained with sgc8 (C); and control cells stained with random DNA (D). Flow cytometry data of target cells stained with sgc8 (green line) and random DNA (black line) (E), and control cells stained with sgc8 (green line) and random DNA (black line) (F). Bar = 80 μm.

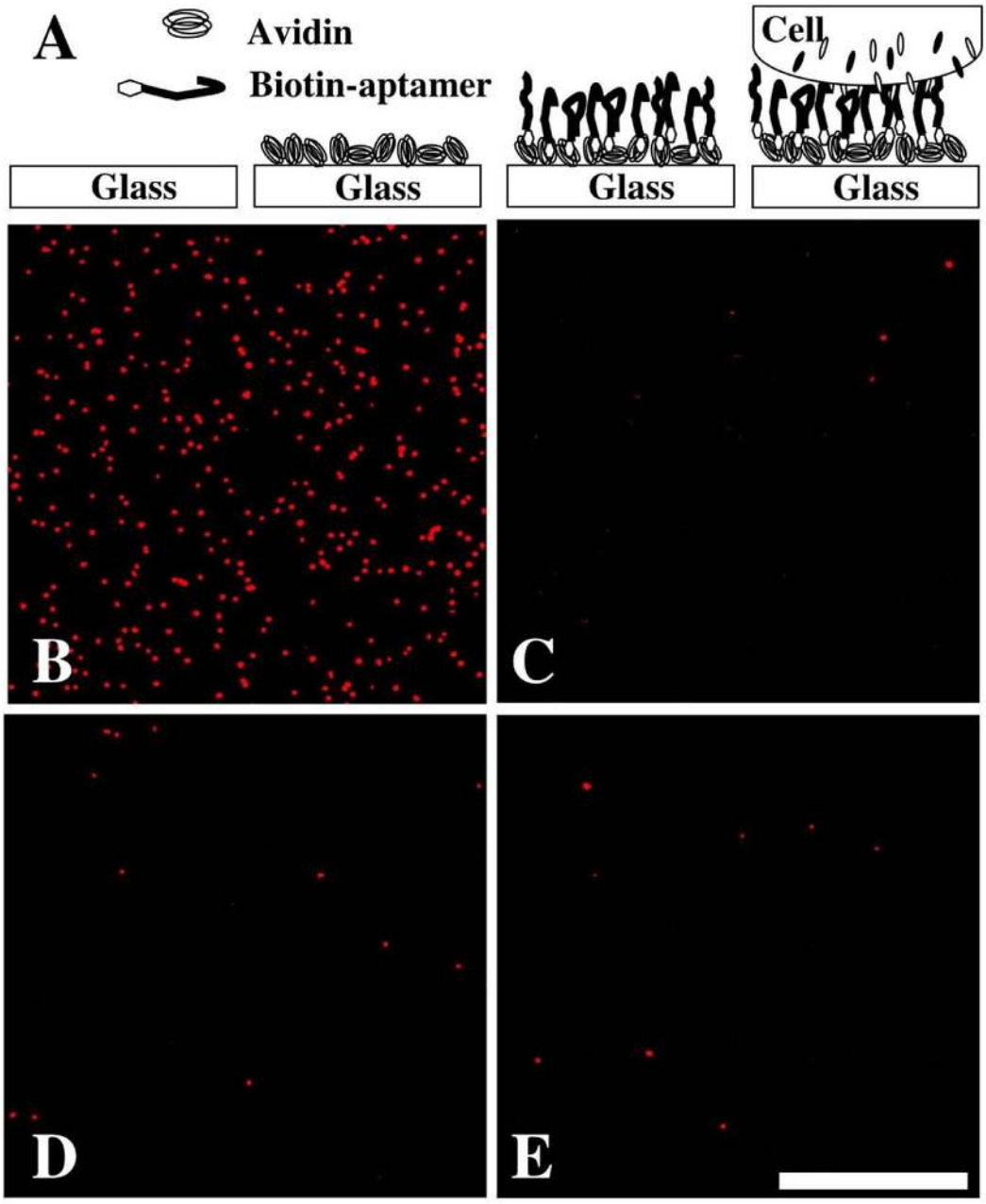


**Fig. 2.**

Surface immobilized sgc8 aptamer selectively captures target cells. Stepwise aptamer immobilization scheme (A). Representative images of cells captured on sgc8 aptamer immobilized surface with target cells at 212 cell/mm$^2$ (B) and control cells at 2 cell/mm$^2$ (C). Representative images of cells captured on random DNA immobilized surface with target cells at 7 cell/mm$^2$ (D) and control cells at 4 cell/mm$^2$ (E). Bar = 500 μm.

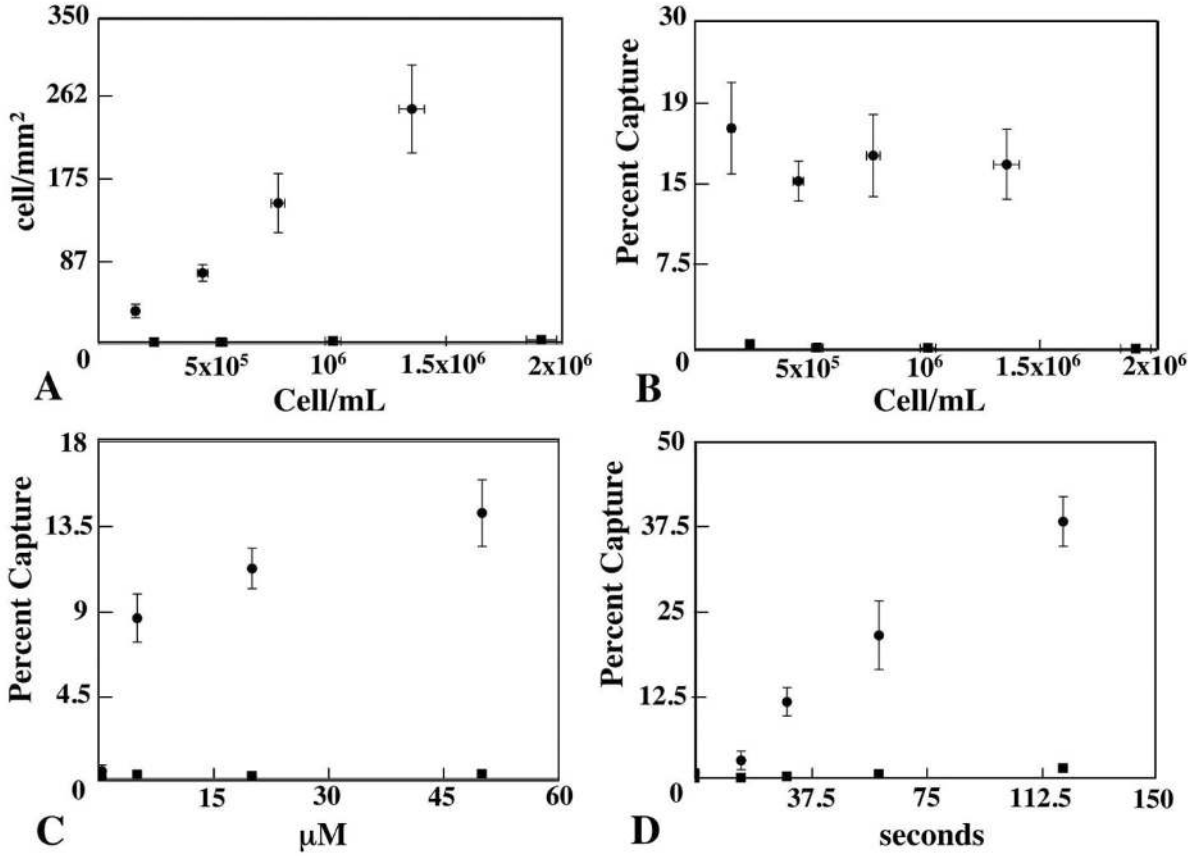


**Fig. 3.**

Response of prototype device to cell capture assay. Target (circle) and control (square) cell surface density increases linearly with increasing cell concentration (A). Cell surface density from (A) converted to percent of capture showing no dependence on cell concentration (B). Increase in percent of capture with increasing concentration of aptamer used during immobilization (C). Percent of capture increases linearly with cell pulse incubation time (D).

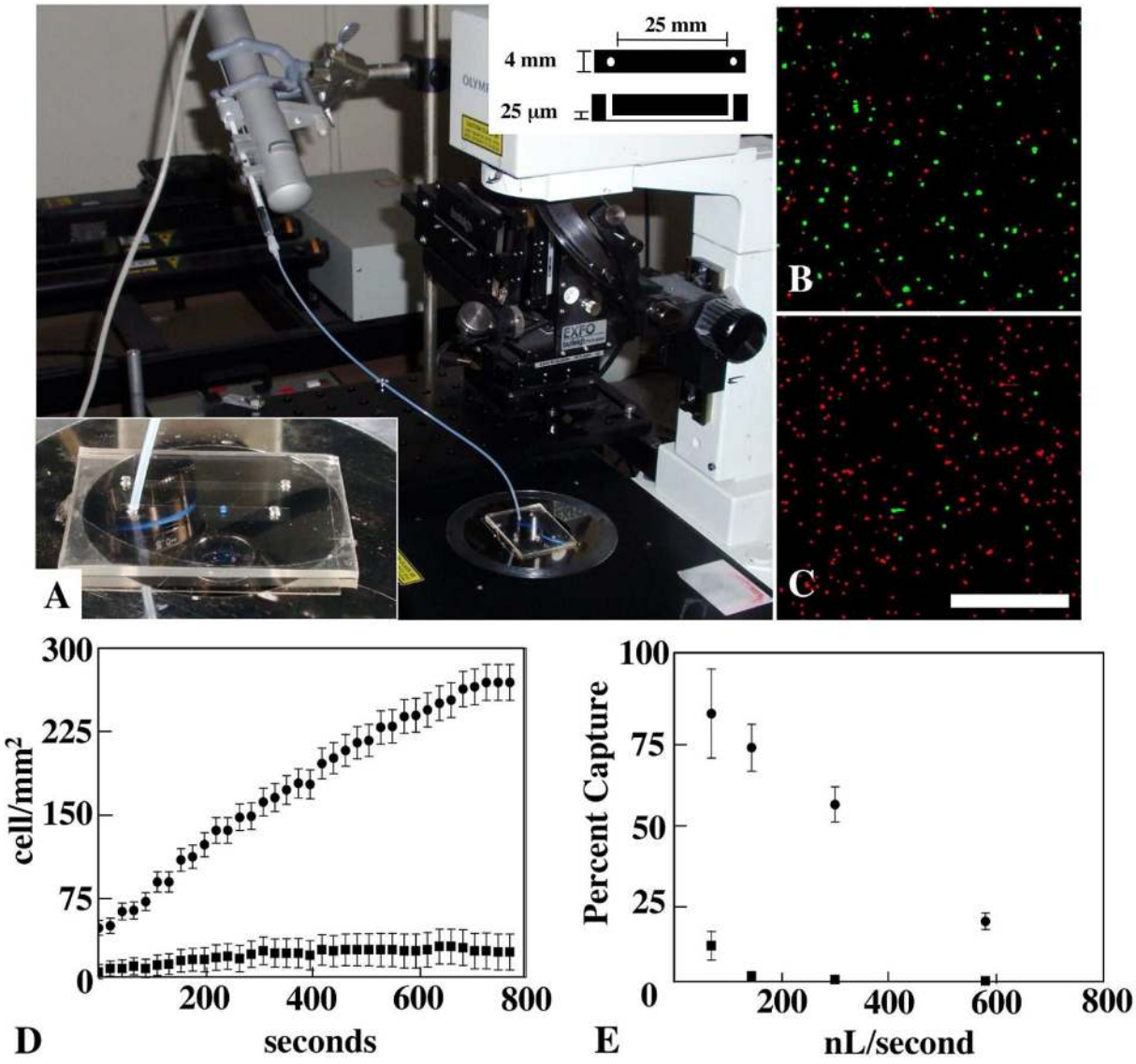


**Fig. 4.**

PDMS device with increased cell capture efficiency. Image of device attached to syringe pump on confocal microscope (A). The bottom left inlay shows the device, and the top right inlay shows top-down and sideways views with dimensions. Representative images of original mixture of cells before cell capture assay (B) and channel surface after the cell capture assay performed at 154 nL/sec flow rate (C), with target and control cells stained red and green, respectively. Cell-surface density measured over the course of the cell capture experiment showing linear increase in target cells captured over time (D). Target cell capture efficiency decreases with increased fluid flow rate (E). Bar = 500 µm.